Journal of Catalysis 271 (2010) 22–32

Contents lists available at ScienceDirect

Journal of Catalysis

journal homepage: www.elsevier.com/locate/jcat

Conversion of cellobiose into sorbitol in neutral water medium over carbon nanotube-supported ruthenium catalysts

Weiping Deng, Mi Liu, Xuesong Tan, Qinghong Zhang *, Ye Wang *

State Key Laboratory of Physical Chemistry of Solid Surfaces, National Engineering Laboratory for Green Chemical Productions of Alcohols, Ethers and Esters, Department of Chemistry, College of Chemistry and Chemical Engineering, Xiamen University, Xiamen 361005, PR China

ARTICLE INFO

Article history:
Received 30 August 2009
Revised 6 January 2010
Accepted 26 January 2010
Available online 24 February 2010

Keywords:
Biomass conversion
Cellobiose
Sorbitol
Ruthenium catalyst
Carbon nanotubes
Hydrogenation
Hydrolysis

ABSTRACT

Carbon nanotube (CNT)-supported ruthenium catalysts were studied for the hydrogenation of cellobiose in neutral water medium. The acidity of catalysts and the size of Ru particles played key roles in the conversion of cellobiose to sorbitol. A higher concentration of nitric acid used for CNT pretreatment provided a better sorbitol yield, suggesting an important role of catalyst acidity. The catalysts with larger mean sizes of Ru particles and abundant acidic sites exhibited better sorbitol yields, while those with smaller Ru particles and less acidic sites favored the formation of 3-β-D-glucopyranosyl-D-glucitol. We elucidated that cellobiose was first converted to 3-β-D-glucopyranosyl-D-glucitol via the hydrogenolysis, and then sorbitol was formed through the cleavage of β-1,4-glycosidic bond in 3-β-D-glucopyranosyl-D-glucitol over the catalysts. The catalyst with smaller Ru particles favored the first step but was disadvantageous to the second step due to the less acidity. Smaller Ru particles also accelerated the degradation of sorbitol.

1. Introduction

The production of fuels and chemicals from renewable biomass resources has attracted much attention in recent years [1–4]. As the most abundant source of biomass and because of the non-edible feature, lignocellulosic biomass may become an important feedstock to replace or partially replace the fossil feedstock for the sustainable production of fuels and chemicals [5–8]. However, the effective utilization of lignocellulosic biomass, which contains cellulose as a main component, is still a challenge because of the robust crystalline structure of cellulose [9,10]. So far, processes for hydrolysis of cellulose to glucose in the presence of strong mineral acids (e.g., H_2SO_4) and for high-temperature pyrolysis or gasification of cellulose to bio-oils or synthesis gas have been developed, but these processes suffer from problems of high-energy input and low selectivity [5–8]. It would be highly desirable to develop a catalytic route for the conversion of cellulose selectively into a platform or building block molecule such as sorbitol, ethylene glycol or 5-hydroxymethylfurfural (HMF) [11], which may be facilely transformed into fuels or chemicals.

A few studies have succeeded in converting cellulose into such a platform molecule under mild conditions [12–16]. The hydrogenation of cellulose in water medium was found to be catalyzed by a Pt/Al_2O_3 catalyst, providing a yield of 31% to hexitols (sorbitol and mannitol, 25% and 6%, respectively) at 463 K [12]. Liu and coworkers [13] developed a two-step transformation of cellulose to polyols catalyzed by reversibly formed acids and activated carbon-supported Ru nanoclusters in hot water, and they obtained a yield of polyols of ~40% (sorbitol, ~30%) at 518 K. Ni-promoted tungsten carbide was demonstrated to catalyze the conversion of cellulose into ethylene glycol with a yield as high as 61% at 518 K [14]. Zhang and coworkers recently developed an effective route for the rapid conversion of cellulose to sugars and further to HMF (HMF yield, ~55%) catalyzed by $CuCl_2/CrCl_2$ catalysts in 1-ethyl-3-methyl-imidazolium chloride solvent at 353–393 K [15]. Very recently, we found that a multi-walled carbon nanotube (CNT)-supported Ru catalyst could catalyze the conversion of cellulose to hexitols with a yield of 40% (sorbitol, 36%) in the presence of H_2 in water medium at 458 K [16]. However, basic understanding of catalyst requirements for the conversion of cellulose is very limited. Undoubtedly, more extensive studies are needed to gain insights into the requirements for the rational design of more efficient catalysts for selective transformations of cellulose.

However, because cellulose is a very complex macromolecule and is insoluble in most solvents, it is not easy to perform fundamental research directly with cellulose. In this context, the fundamental studies with a model molecule would be helpful in the present stage. Cellobiose, which is a D-glucose dimer connected by a β-1,4-glycosidic bond (see Fig. 1 for structural formula), represents the simplest model of cellulose. The studies on catalytic

* Corresponding authors. Fax: +86 592 2183047.
E-mail addresses: zhangqh@xmu.edu.cn (Q. Zhang), wangye@xmu.edu.cn (Y. Wang).

0021-9517/$ - see front matter © 2010 Elsevier Inc. All rights reserved.
doi:10.1016/j.jcat.2010.01.024

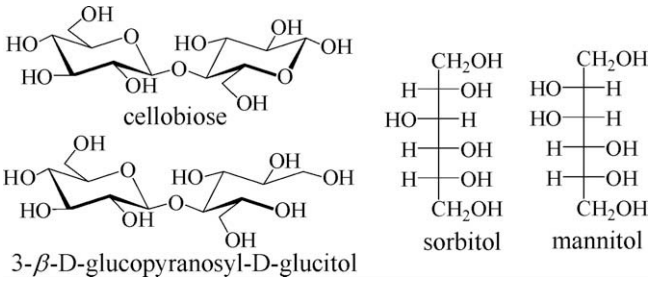

Fig. 1. Structure formulas of cellobiose and some typical products.

conversion of cellobiose may also be useful for transformations of the decrystallized or the soluble oligosaccharides released in hydrothermal or acidic treatments of cellulose, which contain β-1,4-glycosidic bonds. However, there only exist scattered studies on catalytic conversion of cellobiose. Kou and coworkers [17] disclosed that Ru nanoclusters dispersed in water were efficient for the hydrogenation of cellobiose to sorbitol in an acidic aqueous medium (pH = 2.0), whereas under neutral or basic conditions (pH = 7.0 or 10.0), the selectivity of sorbitol was significantly lower. Thus, the protons in the liquid phase might participate in the hydrolysis of cellobiose. Bootsma and Shanks [18] reported that a kind of solid acid catalysts, i.e., organic–inorganic hybrid mesoporous materials containing acidic functional groups, could catalyze the hydrolysis of cellobiose into glucose.

Supported Ru catalysts are known as efficient catalysts for the hydrogenation of glucose to sorbitol [19,20]. The Ru/CNT catalyst was once reported to be more active for the hydrogenation of glucose than the Ru/Al_2O_3 and Ru/SiO_2 [21]. As mentioned earlier, in our preceding work, we found that the Ru/CNT catalyst could efficiently catalyze the conversion of cellulose to sorbitol in the presence of H_2 in water medium [16]. However, there is still little knowledge about the effect of the Ru/CNT catalyst on the conversion of cellulose to sorbitol. Very recently, we chose cellobiose as a model molecule of cellulose and performed detailed studies on catalytic conversion of cellobiose. The present article reports the effects of key factors of Ru/CNT catalysts on the catalytic hydrogenation of cellobiose to sorbitol. We will also discuss the possible reaction mechanism for this catalytic reaction.

2. Experimental

2.1. Catalyst preparation

The CNTs with outer diameters of 20–80 nm and inner diameters of 3–5 nm were prepared by a method reported previously [22]. The prepared CNTs were typically pretreated in concentrated HNO_3 (68 wt.%) at 383 K under refluxing conditions to remove the remaining Ni catalyst used for CNT preparation, the amorphous carbon, and to create function groups (e.g., hydroxyl and carboxylic groups) for anchoring metal precursors [23]. To investigate the role of CNT functionalization, CNTs were also pretreated by HNO_3 with different concentrations (5–68 wt.%) or by concentrated HCl (37 wt.%). No Ni was detected after these pretreatments. Standardly, CNT-supported Ru catalysts were prepared by an impregnation method. The CNTs after pretreatment were added into a $RuCl_3$ aqueous solution and then were dispersed ultrasonically for 0.5 h. After being further stirred for 5 h, the suspension was evaporated at 343 K to remove water. The dried sample was calcined at 623 K in air, followed by H_2 reduction at 623 K for 0.5 h to obtain the Ru/CNT catalyst. The loading of Ru was 1.0 wt.% unless otherwise stated.

We have attempted to prepare Ru/CNT catalysts with different sizes of Ru particles by the impregnation followed by different post-treatments. For this purpose, the dried sample was either directly reduced by H_2 at 623 and 773 K or was first calcined at 623 K in air and then reduced by H_2 at different temperatures (623–773 K). An ethylene glycol reduction method [24] was also applied to the preparation of the Ru/CNT catalysts with different sizes of Ru particles. In this method, $RuCl_3$ was first dissolved in ethylene glycol, and then, the CNTs after pretreatment were added into the $RuCl_3$ solution. After being treated ultrasonically for 0.5 h, the mixture was refluxed at 453 or 483 K for 1 h. The solid product was then recovered by filtration followed by drying.

2.2. Catalyst characterization

Transmission electron microscopy (TEM) measurements were performed on a FEI Tecnai 30 electron microscope (Phillips Analytical) operated at an acceleration voltage of 300 kV. The mean sizes of Ru particles in Ru/CNT samples were estimated from TEM micrographs by counting ca. 150–200 particles. X-ray photoelectron spectra (XPS) were recorded with a Quantum 2000 Scanning ESCA Microprob instrument (Physical Electronics) using Al K_α radiation. The binding energy was calibrated using C_{1s} photoelectron peak at 284.6 eV as a reference. Ru dispersions were measured by H_2—O_2 titration using an ASAP2010C Micromeritics apparatus with the procedures reported in literature [25].

NH_3-temperature-programmed desorption (NH_3-TPD) was performed on a Micromeritics AutoChem 2920 II instrument. Typically, the sample loaded in a quartz reactor was first pretreated with high-purity He at 623 K for 1 h. After the sample was cooled to 393 K, NH_3 adsorption was performed by switching the He flow to a NH_3—He (10 vol.% NH_3) gas mixture and then keeping at 393 K for 1 h. Then, the gas phase or the weakly adsorbed NH_3 was purged by high-purity He at the same temperature. NH_3-TPD was performed in the He flow by raising the temperature to 973 K at a rate of 10 K min^{-1}, and the desorbed NH_3 molecules were detected by ThermoStar GSD 301 T2 mass spectrometer with the signal of $m/e = 16$.

Titration method was also used to evaluate the acidity of Ru/CNT catalysts. In a typical experiment, 0.15 g Ru/CNT catalysts was added into a 25 cm^3 0.01 mol dm^{-3} NaOH aqueous solution and stirred overnight. The mixture was titrated with a 0.01 mol dm^{-3} HCl solution to determine the excess NaOH in the solution to quantify the concentration of the acidic sites on Ru/CNT catalysts. For comparison, the acidity of CNT samples without Ru was also evaluated by the titration method.

2.3. Catalytic reaction

The conversion of cellobiose was performed with a batch-type high-pressure autoclave reactor. Typically, the catalyst (0.050 g) and cellobiose (0.50 mmol) were added into a Teflon-lined stainless steel reactor pre-charged with H_2O (20 cm^3), and then the reaction was carried out at 458 K under 5 MPa H_2 for 3 h. After the reaction, the solid catalyst was separated by centrifugation, and the liquid products were analyzed by a HPLC (Shimazu LC-20A) equipped with a RI detector and a Transgenomic™ CARBON-Sep CHO-620 column (10 μm, 6.5 × 300 mm). The eluent was water with a flow rate of 0.5 cm^3 min^{-1}. The column was thermostated at 338 K by a column heater. Sampling loop has a volume of 20 μL. The pH value of the reaction solution was ~7 after the conversion of cellobiose. Chemicals including sorbitol, mannitol, erythritol [$C_4H_6(OH)_4$], HMF purchased from Alfa Aesar, and glucose, glycerol, ethylene glycol purchased from Sinopharm Chemical Reagent Co. Ltd. were used for calibrations without further treatment. 3-β-D-Glucopyranosyl-D-glucitol synthesized in our laboratory, which was characterized by mass spectroscopy, was also used for the calibration.

3. Results and discussion

3.1. Role of CNT functionalization in catalytic conversion of cellobiose over Ru/CNT catalysts

Because the protons in liquid phase were indispensable for sorbitol formation in the conversion of cellobiose catalyzed by water-dispersed Ru nanoclusters [17], the hydrolysis and hydrogenation were proposed to be two requisite steps for the conversion of cellobiose to sorbitol. To realize the conversion of cellobiose to sorbitol in neutral water medium, we selected Ru supported on acid-functionalized CNTs as the catalyst for this reaction. We prepared Ru/CNT catalysts, in which the CNT was pretreated by the concentrated HCl solution (37 wt.%) or the HNO_3 solutions with concentrations in the range of 5–68 wt.% to generate acidic functional groups [26].

Characterizations with XPS and TEM were performed for this series of catalysts to gain information about the state of Ru species. We did not find significant differences in the chemical state and the mean size of Ru particles in these catalysts. XPS studies revealed that the binding energy of Ru 3d5/2 over each catalyst was around 280.3 eV, suggesting that the Ru species loaded on the CNTs pretreated differently were all in metallic (Ru^0) state [27,28]. Fig. 2 shows the TEM micrographs of the Ru/CNT catalysts with CNTs pretreated by HNO_3 with different concentrations. The size distributions for Ru particles in these catalysts, derived from the TEM micrographs by counting ~150–200 particles, are also shown in Fig. 2. With changing the concentration of HNO_3 used for CNT pretreatment from 5 to 68 wt.%, the mean sizes of Ru particles in these catalysts were almost the same (8.6–8.9 nm).

NH_3-TPD results in Fig. 3 show that almost no desorption of NH_3 occurs over the CNT pretreated by HCl. On the other hand, desorption of NH_3 was observed from the CNTs pretreated by HNO_3, and the peak intensity increased with increasing the concentration of HNO_3. Desorption of NH_3 was also observed from the Ru/CNT catalysts prepared using CNTs pretreated by HNO_3 with different concentrations (Fig. 3B). This indicates that the acidic sites generated on CNT surfaces could be sustained on the prepared Ru/CNT catalysts. Similar phenomenon was observed in our recent studies on the same catalysts for Fischer–Tropsch synthesis [29].

We performed the hydrogenation of cellobiose over the acid-functionalized Ru/CNT catalysts. As shown in Fig. 4, the Ru/CNT could catalyze the formation of sorbitol from cellobiose at 458 K, and the catalytic performance depended on the acid used for CNT pretreatment. Sorbitol yield was only 26% when the CNT pretreated by HCl (37 wt.%) was used as the support of Ru catalyst. Sorbitol yield rose from 56% to 87% when the concentration of HNO_3 for CNT pretreatment increased from 5 wt.% to 68 wt.%. Therefore, the acidity generated on CNTs during the pretreatment by concentrated HNO_3 plays an important role in the conversion of cellobiose to sorbitol. This result is in essence the same with that obtained in our previous studies for the conversion of cellulose to sorbitol [16]. The following studies have been focused on the catalysts using the CNT pretreated by 68 wt.% HNO_3 as the support.

To gain further information on the conversion of cellobiose to sorbitol, we have investigated the temperature dependence of product distributions for cellobiose conversion over the Ru/CNT catalyst with the CNT pretreated by 68 wt.% HNO_3. Fig. 5 shows that 3-β-D-glucopyranosyl-D-glucitol is formed as the main product at lower temperatures, and it is transformed to sorbitol with increasing the reaction temperature up to 458 K. A further higher temperature favored the formation of degradation products including $C_6H_{10}(OH)_4$, $C_4H_6(OH)_4$, $C_3H_5(OH)_3$, $C_2H_4(OH)_2$, and CH_4. From these results, we suggest that 3-β-D-glucopyranosyl-D-glucitol may be an important intermediate for sorbitol formation from cellobiose over the Ru/CNT catalyst.

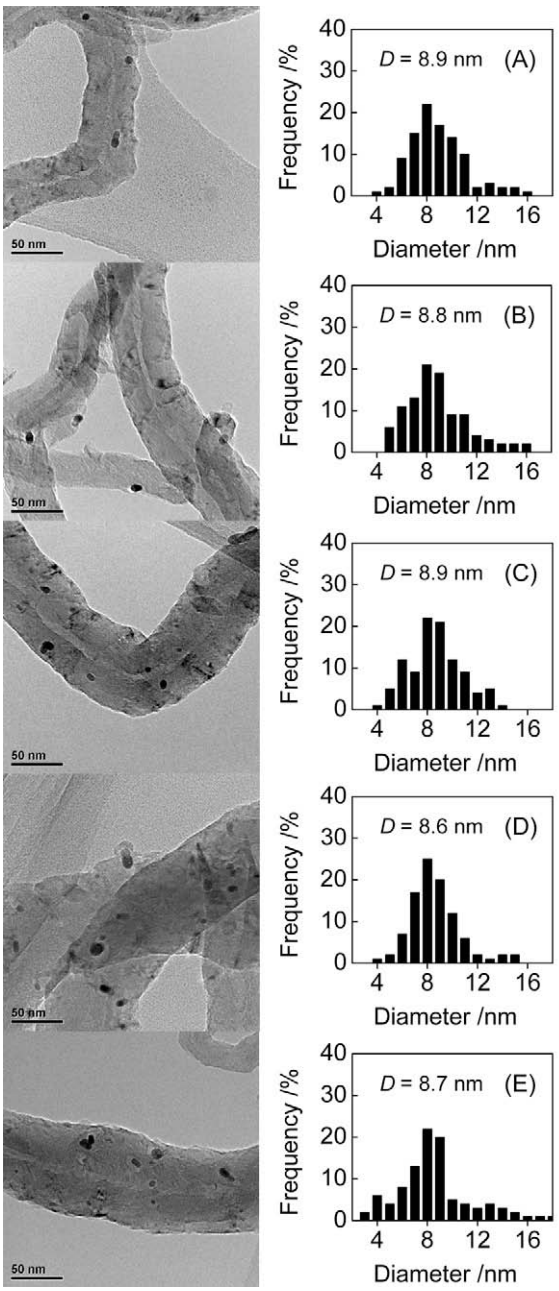

Fig. 2. TEM micrographs and Ru particle size distributions of the Ru/CNT catalysts with CNTs pretreated by HNO_3 with different concentrations. Concentration of HNO_3 used for CNT pretreatment: (A) 5 wt.%, (B) 19 wt.%, (C) 37 wt.%, (D) 52 wt.%, and (E) 68 wt.%.

3.2. Ru/CNT catalysts with different sizes of Ru particles and their catalytic behaviors

3.2.1. Preparation of Ru/CNT catalysts with different sizes of Ru particles

Besides the acidity of the catalyst, Ru nanoparticles are believed to play important roles in the formation of sorbitol from cellobiose. Because the size of metal nanoparticles is one of the most important factors dominating the performances of nanoparticles-based catalysis [30], we have prepared a series of Ru/CNT samples with

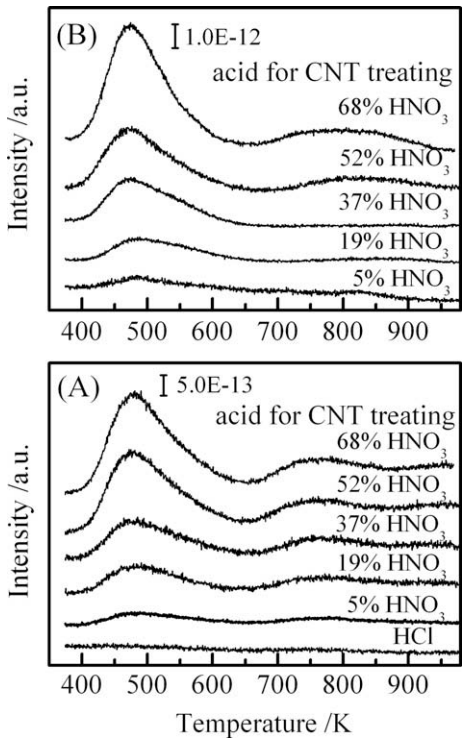

Fig. 3. NH_3-TPD profiles of the CNTs pretreated by concentrated HCl or by HNO_3 with different concentrations (A) and the Ru/CNT catalysts prepared using CNTs pretreated by HNO_3 with different concentrations (B).

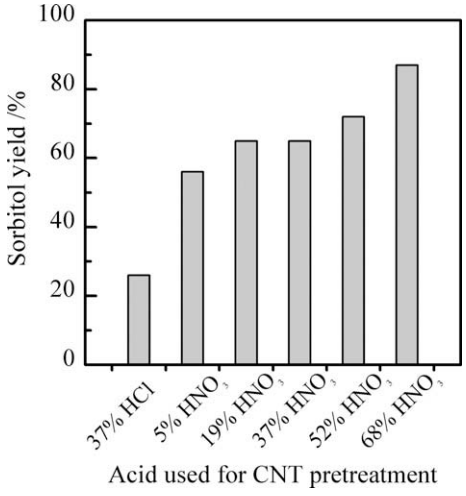

Fig. 4. Sorbitol yield in the conversion of cellobiose over the Ru/CNT catalysts prepared using CNTs pretreated by concentrated HCl or by HNO_3 with different concentrations. Reaction conditions: cellobiose, 0.50 mmol; catalyst, 0.050 g; H_2O, 20 cm^3; H_2, 5 MPa; temperature, 458 K; time, 3 h.

different mean sizes of Ru particles to clarify the size effect in the Ru/CNT-catalyzed conversion of cellobiose. With TEM observations, we clarified that the direct H_2 reduction at 773 K without calcination resulted in smaller Ru nanoparticles finely dispersed on the CNT surfaces (Fig. 6A, Ru/CNT-H773). The mean size of Ru (D) in this sample estimated from TEM images by counting ca. 150–200 particles was 2.4 nm. The size of Ru particles increased significantly if the calcination at 623 K was adopted before H_2 reduction. Moreover, a change of the temperature for H_2 reduction could change the mean size of Ru particles. The catalysts with mean sizes of Ru particles at 8.7 and 12 nm were obtained by using

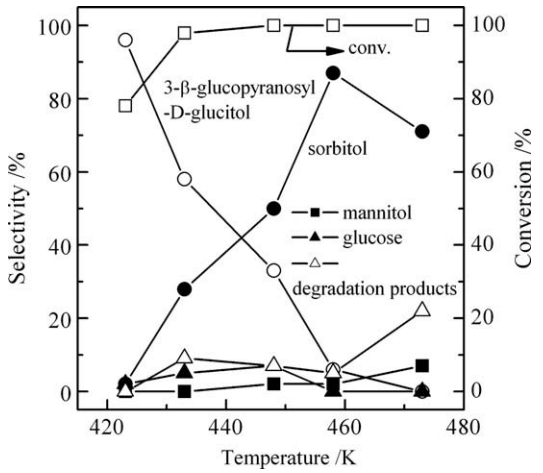

Fig. 5. Dependence of catalytic performances with reaction temperature for the conversion of cellobiose over the Ru/CNT catalyst with a mean size of Ru particles at 8.7 nm. Reaction conditions: cellobiose, 0.50 mmol; catalyst, 0.050 g; H_2O, 20 cm^3; H_2, 5 MPa; time, 3 h.

reduction temperatures of 623 K (Fig. 6B, Ru/CNT-C623-H623) and 773 K (Fig. 6C, Ru/CNT-C623-H773), respectively. On the other hand, Ru/CNT catalysts with mean sizes of Ru particles at 5.1 and 6.8 nm could be obtained by using the method of ethylene glycol reductions at 483 K (Fig. 6D, Ru/CNT-EG483) and 453 K (Fig. 6E, Ru/CNT-EG453), respectively. In short, we have succeeded in preparing the Ru/CNT catalysts with mean sizes of Ru particles varying from 2.4 to 12 nm.

3.2.2. Acidity of the prepared Ru/CNT catalysts with different sizes of Ru particles

From the results described previously, we know that the formation of sorbitol is affected by the catalyst acidity, which arises from the CNT pretreatment by concentrated HNO_3. Therefore, we have evaluated the acidity of the prepared Ru/CNT catalysts with different mean sizes of Ru particles by both the NH_3-TPD and the titration methods.

Fig. 7 shows the NH_3-TPD profiles of these catalysts. Only a lower-temperature NH_3 desorption peak (~480 K) was observed for the Ru/CNT catalyst with a mean size of Ru particles at 2.4 nm, and the intensity of this peak was lower than that for other catalysts. Moreover, for the catalysts with mean sizes of Ru particles $\geqslant$5.1 nm, in addition to the lower-temperature peak, another NH_3 desorption peak at higher temperatures (>700 K) could be observed, indicating the presence of acid sites with stronger acidity, and the peak associated with the stronger acid sites further shifts to higher temperatures over the samples with Ru particles at 8.7 nm or 12 nm. From these NH_3-TPD results, it becomes clear that there exist differences in the acidity among the Ru/CNT catalysts with different mean sizes of Ru particles. When compared to the Ru/CNT catalysts with larger Ru particles, the Ru/CNT catalyst with a mean size of Ru particles at 2.4 nm (Ru/CNT-H773) possesses much lower acidity. This observation has further been confirmed by the result obtained from the titration method. As shown in Table 1, the amount of acidic sites for the Ru/CNT-H773 (2.4 nm) catalyst was significantly lower than those for the other Ru/CNT catalysts. The amounts of acidic sites over the CNTs alone, which underwent post-treatments with the same procedures as those for the preparation of the Ru/CNT catalysts with different Ru sizes, were also measured by the titration method. When compared to the CNTs after different post-treatments, unexpectedly, the Ru/CNT catalysts showed larger amounts of acidic sites.

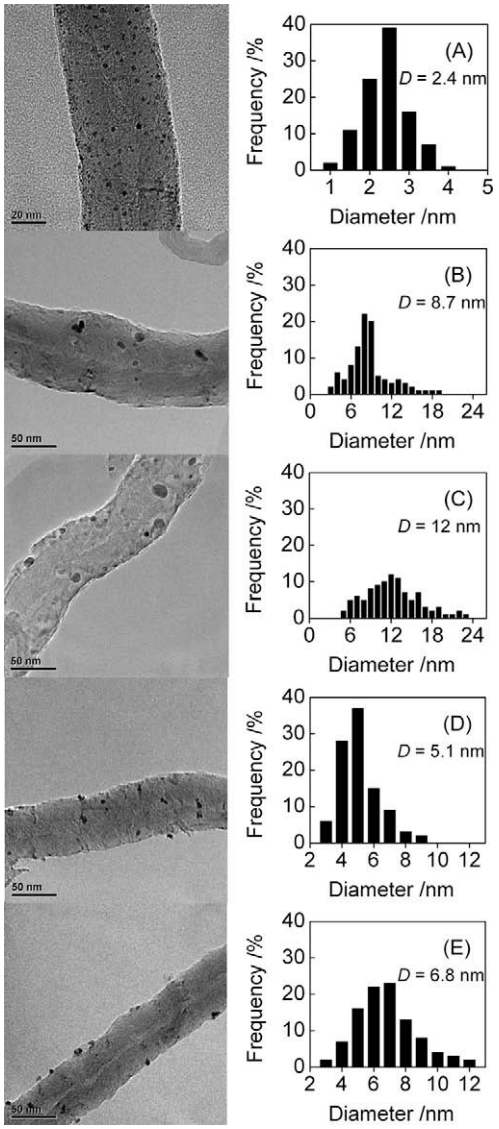

Fig. 6. TEM micrographs and Ru particle size distributions of the Ru/CNT catalysts prepared by the impregnation (A–C) and the ethylene glycol reduction (D and E) methods. (A) Direct reduction by H_2 at 773 K after impregnation (without calcination); (B) and (C) with calcination at 623 K after impregnation, followed by H_2 reductions at 623 and 773 K, respectively; (D) and (E) reductions by ethylene glycol at 483 and 453 K, respectively.

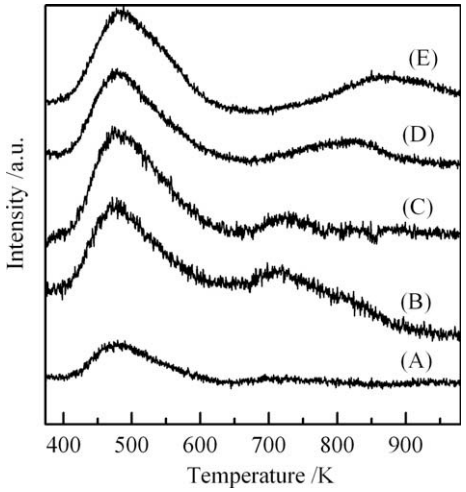

Fig. 7. NH_3-TPD profiles of the Ru/CNT catalysts with different mean sizes of Ru particles. (A) Ru/CNT-H773 (Ru, 2.4 nm); (B) Ru/CNT-EG483 (Ru, 5.1 nm); (C) Ru/CNT-EG453 (Ru, 6.8 nm); (D) Ru/CNT-C623-H623 (Ru, 8.7 nm); (E) Ru/CNT-C623-H773 (Ru, 12 nm).

Table 1
Amount of acidic sites over the CNTs after different post-treatments and the Ru/CNT samples with different mean sizes of Ru particles.[a]

Sample[b]	Mean size of Ru (nm)	Amount of acidic sites (mmol g^{-1})
CNT-H773	–	0.12
CNT-EG483	–	0.20
CNT-EG453	–	0.22
CNT-C623-H623	–	0.25
CNT-C623-H773	–	0.17
Ru/CNT-H773	2.4	0.37
Ru/CNT-EG483	5.1	0.50
Ru/CNT-EG453	6.8	0.55
Ru/CNT-C623-H623	8.7	0.56
Ru/CNT-C623-H773	12	0.51

[a] Measured by the titration method.
[b] The numbers after H, C, and EG denote temperatures for H_2 reduction, calcination and ethylene glycol reduction, respectively (also see the main text).

Although the reason for the differences in the acidity among the Ru/CNT catalysts with different Ru sizes and the CNTs is still unclear at this moment, the acidity of our catalysts is believed to stem from the oxygen-containing functional groups on CNT surfaces generated during the HNO_3 pretreatment or the post-treatments. Several groups [31–33] reported that the analysis of O1s XPS spectra could give useful information on the functional groups on CNT surfaces. For example, it was proposed that the O1s peak with binding energies at 531.1, 532.3, 533.3, and 534.2 eV could be attributed to the carbonyl groups, the carbonyl oxygen atoms in esters and anhydrides or the oxygen atoms in hydroxyls or ethers, the ether oxygen atoms in esters and anhydrides, and the oxygen atoms in carboxylic groups, respectively [32–34]. Thus, we have performed XPS studies for our catalysts with different mean sizes of Ru particles, and the results are shown in Fig. 8. The broad feature of O1s peak in Fig. 8 implies that several types of oxygen-containing functional groups co-exist on our catalysts. The results derived from the deconvolution of O1s peaks are summarized in Table 2. The percentage of the composition at a binding energy of 534.2 eV, which could be ascribed to the acidic carboxylic group on the CNT surface, increased from 8.8% to 16%, 17%, 22%, and 18% when the mean size of Ru particles rose from 2.4 to 5.1, 6.8, 8.7, and 12 nm, respectively. These results further suggest that the catalyst with a mean size of Ru particles at 2.4 nm possesses less acid sites. However, from Table 2, the differences in the fraction of the acidic carboxylic groups among the catalysts with other mean sizes of Ru particles are not very significant. Moreover, it is still difficult to explain the differences in the peak positions of the higher-temperature peak observed in NH_3-TPD profiles among the catalysts with different mean sizes of Ru particles (Fig. 7).

3.2.3. Catalytic conversions of cellobiose to sorbitol over Ru/CNT catalysts

Fig. 9 shows the catalytic performances of the Ru/CNT catalysts with different mean sizes of Ru for the conversion of cellobiose at 458 K for 3 h. The catalyst with a smaller mean size of Ru (2.4 nm) showed a lower sorbitol yield. The sorbitol yield increased with increasing the mean size of Ru particles up to 8.7 nm, and a further increase in the mean size of Ru particles to 12 nm only slightly changed sorbitol yield. 3-β-D-Glucopyranosyl-D-glucitol, mannitol, and degradation products (including $C_6H_{10}(OH)_4$, $C_4H_6(OH)_4$,

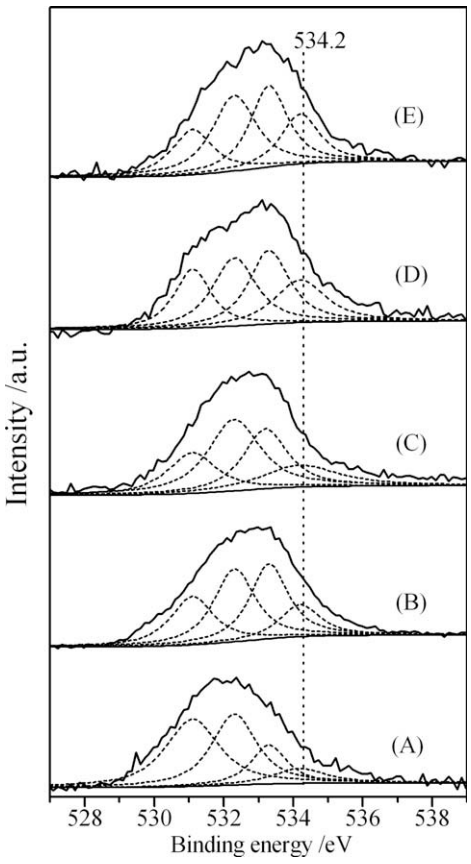

Fig. 8. O1s XPS spectra of the Ru/CNT catalysts with different mean sizes of Ru particles. The dotted lines are deconvolution results. (A) Ru/CNT-H773 (Ru, 2.4 nm); (B) Ru/CNT-EG483 (Ru, 5.1 nm); (C) Ru/CNT-EG453 (Ru, 6.8 nm); (D) Ru/CNT-C623-H623 (Ru, 8.7 nm); and (E) Ru/CNT-C623-H773 (Ru, 12 nm).

$C_3H_5(OH)_3$, and $C_2H_4(OH)_2$) were formed with higher yields over the catalysts with smaller Ru particles (<8.7 nm). These observations suggest that the mean size of Ru nanoparticles is one of the important factors, which influence the conversion of cellobiose into sorbitol. However, the acidity of these catalysts is different as shown in Table 1, Figs. 7 and 8, while the result in Fig. 4 has indicated the important role of acidity in the formation of sorbitol. The contribution of acidity in these catalysts will be discussed in Section 3.3.3.

We have performed the recycling uses of the Ru/CNT-C628-H628 (Ru, 8.7 nm) catalyst, which can provide the highest sorbitol yield. No decreases in sorbitol yield were observed in the repeated uses, and a sorbitol yield of 88% was obtained after four recycling tests. Thus, our Ru/CNT catalyst could be used repeatedly.

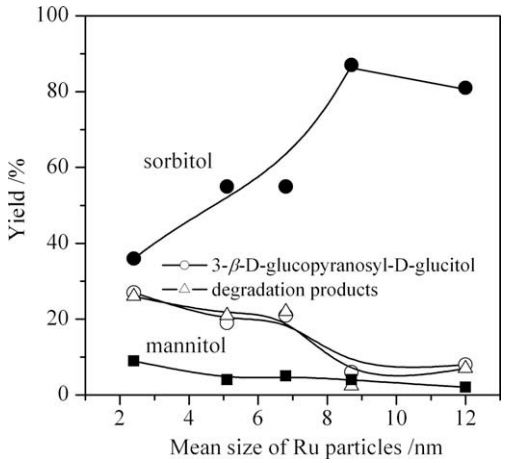

Fig. 9. Product yields in the conversion of cellobiose over the Ru/CNT catalysts with different mean sizes of Ru particles. Reaction conditions: cellobiose, 0.50 mmol; catalyst, 0.050 g; H_2O, 20 cm^3; H_2, 5 MPa; temperature, 458 K; time, 3 h.

3.3. Possible reaction mechanism for the conversion of cellobiose over Ru/CNT catalysts

3.3.1. Reaction pathways

To understand the possible reaction pathways for the conversion of cellobiose over the Ru/CNT catalysts, we performed kinetic studies. Fig. 10 shows the time courses for cellobiose conversions over the Ru/CNT catalysts with mean sizes of Ru particles at 2.4, 5.1, 8.7, and 12 nm. Over all of these catalysts, it is found that 3-β-D-glucopyranosyl-D-glucitol is formed as the main product at the initial reaction stage. The yield of 3-β-D-glucopyranosyl-D-glucitol could reach 93% over the catalyst with a mean size of Ru particles at 2.4 nm after 20 min of reaction (Fig. 10A). With prolonging the reaction time, the yield of sorbitol, the target product, increased significantly along with a decrease in that of 3-β-D-glucopyranosyl-D-glucitol, indicating that sorbitol was formed from the consecutive conversion of 3-β-D-glucopyranosyl-D-glucitol. For the Ru/CNT catalysts with mean Ru sizes of 8.7 (Fig. 10C) and 12 nm (Fig. 10D), the yield of sorbitol could reach 80–90%, while the highest sorbitol yields were lower than ~40% and ~60% over the catalysts with mean Ru sizes of 2.4 nm (Fig. 10A) and 5.1 nm (Fig. 10B), respectively. The lower yield of sorbitol over the Ru/CNT catalysts with smaller Ru particles was likely due to the rapid conversion of sorbitol consecutively to mannitol and other degradation products over these catalysts. Glucose was formed with very lower yields (<5%) over all of the catalysts in Fig. 10, except for that over the Ru/CNT-C623-H773 catalyst with a larger mean size of Ru (12 nm), where a relatively higher yield of glucose (~20%) could be achieved at the initial reaction stage (Fig. 10D). These observations strongly suggest that the main reaction in the

Table 2
Deconvolution results of XPS O1s peaks for the Ru/CNT catalysts with different mean sizes of Ru particles.

Catalyst	Mean sizes of Ru (nm)	Fraction of each O1s component (%)			
		531.1 eV[a]	532.3 eV[b]	533.3 eV[c]	534.2 eV[d]
Ru/CNT-H773	2.4	40	35	16	8.8
Ru/CNT-EG483	5.1	11	43	30	16
Ru/CNT-EG453	6.8	20	37	26	17
Ru/CNT-C623-H623	8.7	19	27	32	22
Ru/CNT-C623-H773	12	12	46	24	18

[a] The C=O groups at 531.1 eV.
[b] The carbonyl oxygen atoms in esters, amides, anhydrides or oxygen atoms in hydroxyls or ethers at 532.3 eV.
[c] The ether oxygen atoms in esters and anhydrides at 533.3 eV.
[d] The oxygen atoms in carboxyl groups at 534.2 eV.

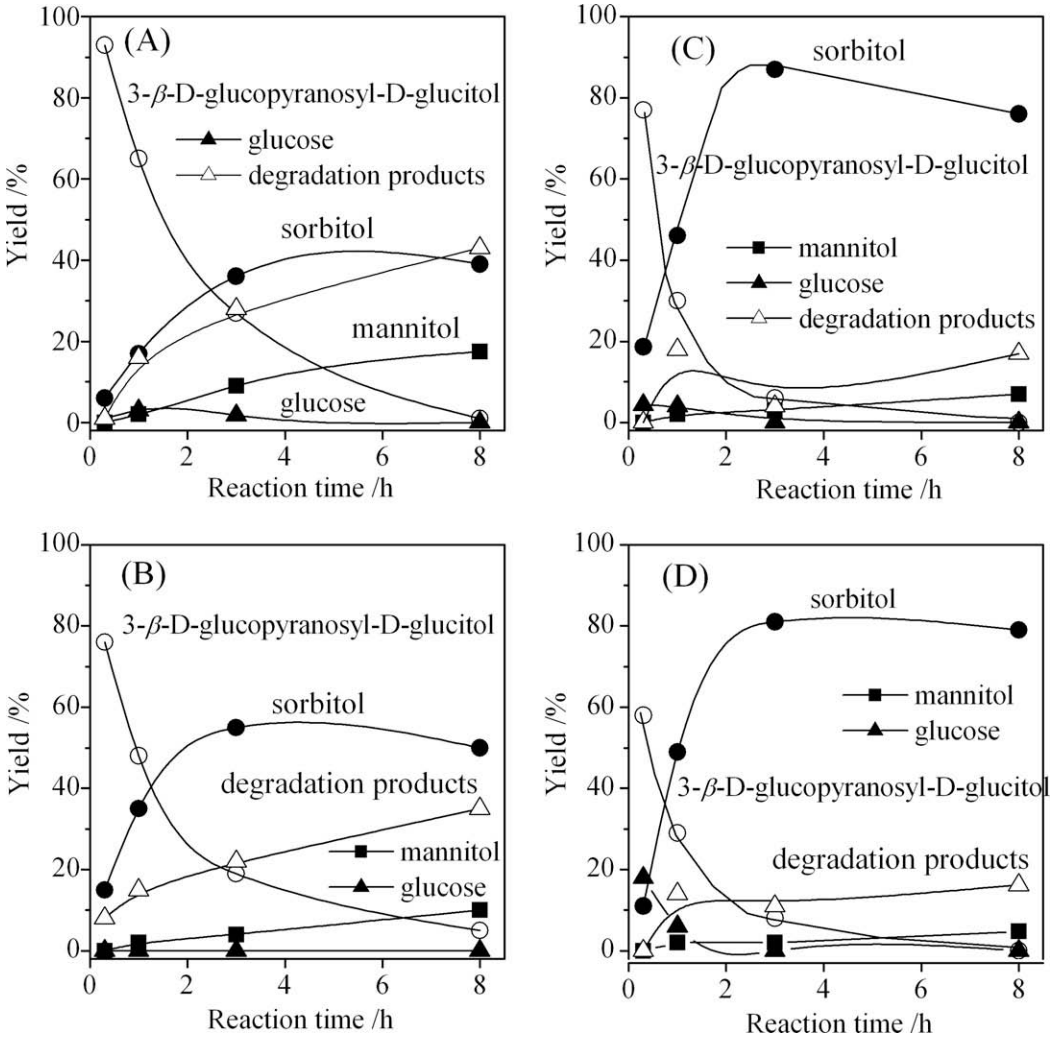

Fig. 10. Time courses for the conversions of cellobiose over the Ru/CNT catalysts with different mean sizes of Ru particles. (A) Ru/CNT-H773 (Ru, 2.4 nm); (B) Ru/CNT-EG483 (Ru, 5.1 nm); (C) Ru/CNT-C623-H623 (Ru, 8.7 nm); and (D) Ru/CNT-C623-H773 (Ru, 12 nm). Reaction conditions: cellobiose, 0.50 mmol; catalyst, 0.050 g; H_2O, 20 cm^3; H_2, 5 MPa; temperature, 458 K.

first step for cellobiose conversions over the Ru/CNT catalysts is the formation of 3-β-D-glucopyranosyl-D-glucitol via the hydrogenolysis of the C—O bond in one glucose ring but not the formation of glucose by the cleavage of the β-1,4-glycosidic bond. Over Ru/CNT catalysts with smaller Ru particles, it is hard to obtain high sorbitol yield because of its rapid degradation.

On the basis of these results, we propose reaction pathways for the conversion of cellobiose in Fig. 11. Over the Ru/CNT catalysts, 3-β-D-glucopyranosyl-D-glucitol is first formed by the hydrogenolysis of cellobiose as the main primary product (Step I). Only over the catalyst with a larger mean size of Ru particles (12 nm), where the hydrogenation activity of the Ru particles may be not very high, glucose can be formed as a minor primary product through hydrolysis catalyzed by the acid sites (Step I′). The subsequent transformation of 3-β-D-glucopyranosyl-D-glucitol may provide a mole of glucose together with the formation of sorbitol through hydrolysis (Step II). However, we only detected a small amount of glucose in our systems (Figs. 5 and 10). This allows us to speculate that glucose may be converted to sorbitol very rapidly over the Ru/CNT catalysts under the current reaction conditions (Step III). This has been confirmed by the experimental results for the conversion of glucose over the Ru/CNT catalysts (Table 3). The hydrogenation of glucose to sorbitol, mannitol, and a small amount of other degradation products could be completed even in 10 min over the Ru/CNT catalysts with any mean size of Ru particles (Step IV and Step V).

The reaction pathways we have proposed in Fig. 11 are quite different from those suggested in a previous study [17]. During cellobiose conversions over Ru particles dispersed in neutral aqueous solutions (pH = 7), Kou and coworkers [17] also found the formations of 3-β-D-glucopyranosyl-D-glucitol (major product) and sorbitol (minor product). However, they suggested that the formation of sorbitol had no relations with the 3-β-D-glucopyranosyl-D-glucitol formed. Instead, they proposed that sorbitol was formed by the cleavage of β-1,4-glycosidic bond through the direct hydrogenation of cellobiose based on the dideoxyhexitol detected. In our work, although dideoxyhexitol has really been detected as a minor product (selectivity, ~1%) over some Ru/CNT catalysts, our results in Figs. 5 and 10 clearly indicate that the consecutive conversion of 3-β-D-glucopyranosyl-D-glucitol is the main path for sorbitol formation. We speculate that the very small amount of dideoxyhexitol may be formed by the consecutive dehydroxylation of sorbitol.

3.3.2. Rate of cellobiose conversion over Ru/CNT catalysts

To gain information about the functions of the Ru/CNT catalyst in each reaction steps in Fig. 11, we have investigated the intrinsic

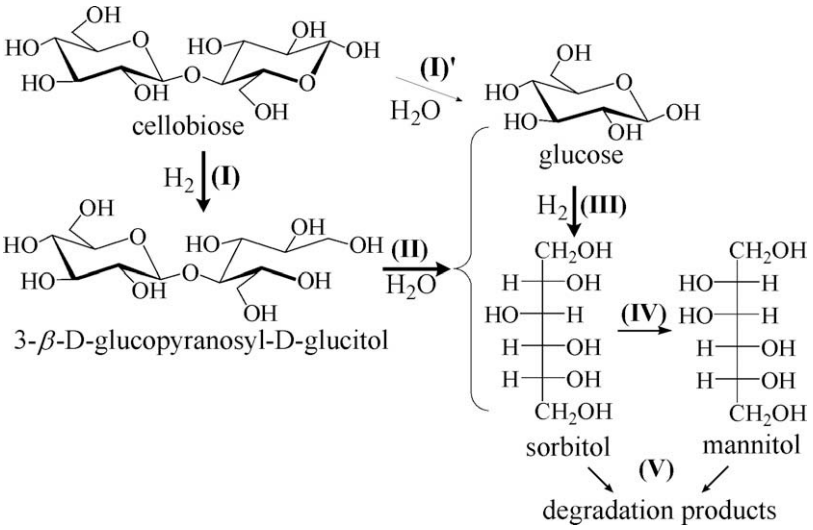

Fig. 11. Proposed reaction pathways for the conversion of cellobiose over the Ru/CNT catalysts.

Table 3
Hydrogenation of glucose over the Ru/CNT catalysts with different mean sizes of Ru nanoparticles.[a]

Catalyst	Mean size of Ru (nm)	Conversion (%)	Selectivity (%)	
			Sorbitol	Mannitol
Ru/CNT-H773	2.4	100	86	4.0
Ru/CNT-EG483	5.1	100	86	3.6
Ru/CNT-C623-H623	8.7	100	87	1.0
Ru/CNT-C623-H773	12	100	88	2.0

[a] Reaction conditions: glucose, 1.0 mmol; catalyst, 0.050 g; H_2, 5 MPa; H_2O, 20 cm^3; temperature, 458 K; time, 10 min.

activities of our catalysts in cellobiose conversions. To obtain the genuine activity of each catalyst, we have chosen reaction conditions (relatively milder temperature) to keep a relatively low cellobiose conversion. Within initial 30 min at 423 K over the Ru/CNT catalysts (Fig. 12), the main product for cellobiose conversions was 3-β-D-glucopyranosyl-D-glucitol. We have also examined in detail the blank reactions and the reactions over the CNTs after different post-treatments similar to those used for the preparation of Ru/CNT catalysts with different mean Ru sizes. The results summarized in Table 4 show that the blank reaction does not occur under the conditions of Table 4. CNTs could provide a small amount of glucose and HMF probably due to the hydrolysis of cellobiose to glucose and the subsequent dehydration of glucose to HMF over the acidic sites on CNTs. However, no 3-β-D-glucopyranosyl-D-glucitol or sorbitol was formed over the CNTs alone. Thus, we can conlcude that Ru nanoparticles are responsible for the formations of 3-β-D-glucopyranosyl-D-glucitol and sorbitol. From the relationship between the conversion and the reaction time in Fig. 12A, the rate of cellobiose conversion has been calculated, and the results are summarized in Table 5. The conversion rate decreased significantly with increasing the mean size of Ru particles. Because Ru is expected to catalyze the hydrogenation of cellobiose to 3-β-D-glucopyranosyl-D-glucitol, we have evaluated the turnover frequency (TOF) for each catalyst on the basis of the rate of cellobiose conversion per surface Ru atom. The dispersion of Ru, i.e., the fraction of surface Ru atoms in the whole Ru atoms, was measured by a H_2—O_2 titration technique [25]. The value thus measured was in good agreement with the results estimated from the size of Ru particles by the following equation assuming spherical Ru particles: dispersion = 1.32/D (nm), where D is the mean size of Ru particles

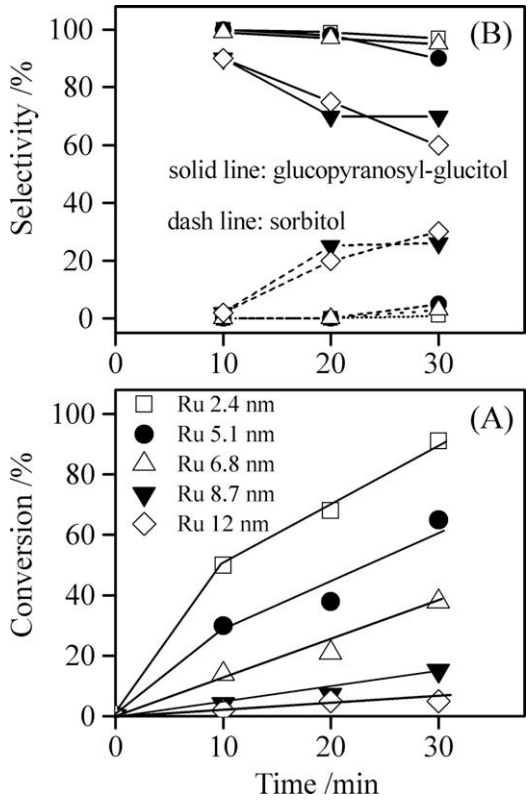

Fig. 12. Catalytic behaviors for the conversion of cellobiose at the initial stage over the Ru/CNT catalysts with different mean sizes of Ru particles. (A) Conversion and (B) selectivity. Reaction conditions: cellobiose, 0.79 mmol; catalyst, 0.020 g; H_2O, 20 cm^3; H_2, 2 MPa; temperature, 423 K.

measured by TEM [34]. As shown in Table 5, the catalysts with smaller mean sizes of Ru particles (2.4 and 5.1 nm) exhibited higher TOFs. In other words, these two catalysts are more active toward the conversion of cellobiose to 3-β-D-glucopyranosyl-D-glucitol (i.e., hydrogenolysis of the C—O bond of one glucose ring, see Step I in Fig. 11). Smaller metal particles are generally believed to possess larger fractions of coordinately unsaturated Ru atoms. Our present result indicates that the coordinately unsaturated Ru atoms are more active toward the hydrogenolysis of cellobiose.

Table 4
Conversions of cellobiose in the blank reactions and the reactions over CNTs after different post-pretreatments and Ru/CNTs with different mean sizes of Ru particles.[a]

Sample	Mean size of Ru (nm)	Cellobiose conversion (%)	Yield (%)			
			Sorbitol	Glucose	HMF	Glucitol[b]
Blank	–	<0.1	0	0	0	0
CNT-H773	–	1	0	0.8	0.1	0
CNT-EG483	–	5	0	2.4	1.4	0
CNT-EG453	–	5	0	3	1.2	0
CNT-C623-H623	–	7	0	2.9	4	0
CNT-C623-H773	–	4	0	2	2	0
Ru/CNT-H773	2.4	91	1	0	0	88
Ru/CNT-EG483	5.1	65	2	0	0	58
Ru/CNT-EG453	6.8	38	2	0	0	36
Ru/CNT-C623-H623	8.7	15	4	0	0	11
Ru/CNT-C623-H773	12	5	2	0	0	3

[a] Reaction conditions: cellobiose, 0.79 mmol; catalyst, 0.020 g; H_2O, 20 cm^3; H_2, 2 MPa; temperature, 423 K; time, 30 min.
[b] Glucitol denotes 3-β-D-glucopyranosyl-D-glucitol.

Table 5
Rate and turnover frequency for cellobiose conversions at initial reaction stage over the Ru/CNT catalysts with different mean sizes of Ru particles.

Catalyst	Mean size of Ru (nm)	Ru dispersion[a]	Ru dispersion[b]	Cellobiose conversion rate[c] (mmol g_{cat}^{-1} h^{-1})	TOF[d] (10^{-3} s^{-1})
Ru/CNT-H773	2.4	0.52	0.55	98.4	532
Ru/CNT-EG483	5.1	0.24	0.26	45.6	533
Ru/CNT-EG453	6.8	0.17	0.19	30.4	500
Ru/CNT-C623-H623	8.7	0.15	0.15	12.0	222
Ru/CNT-C623-H773	12	0.11	0.11	6.4	163

[a] Measured from a H_2—O_2 titration technique [25].
[b] Calculated by the following equation: dispersion = 1.32/D (nm).
[c] Calculated using the data in Fig. 12A.
[d] Evaluated on the basis of the rate of cellobiose conversion per surface Ru atom by using Ru dispersion measured from H_2—O_2 titration technique.

3.3.3. Rate of 3-β-D-glucopyranosyl-D-glucitol conversion over Ru/CNT catalysts

Similar studies were performed using 3-β-D-glucopyranosyl-D-glucitol as a reactant to gain information about Step II in Fig. 11. Because the hydrolysis over the Ru/CNT catalysts proceeds not as quickly as the hydrogenolysis step (Step I in Fig. 11), relatively strict reaction conditions have been employed for the conversion of 3-β-D-glucopyranosyl-D-glucitol. As shown in Fig. 13A, over different Ru/CNT catalysts, the conversions of 3-β-D-glucopyranosyl-D-glucitol all increased almost proportionally to the reaction time in 120 min, and sorbitol was the main product (Fig. 13B). The rates of 3-β-D-glucopyranosyl-D-glucitol conversions calculated from Fig. 13A are summarized in Table 6. The combination of the results in Table 6 and Fig. 7 or Table 1 suggests that the acidity of the catalysts play an important role in the transformation of 3-β-D-glucopyranosyl-D-glucitol to sorbitol and glucose (Step II in Fig. 11). Almost no glucose was observed during these experiments because glucose could be subsequently converted to sorbitol over Ru particles very rapidly (Step III). Thus, the higher acidity of the catalyst results in a higher rate of 3-β-D-glucopyranosyl-D-glucitol conversion via the cleavage of the β-1,4-glycosidic bond.

The distribution of the products (Fig. 13B) showed that the selectivity of sorbitol produced from the conversion of 3-β-D-glucopyranosyl-D-glucitol varied largely over different Ru/CNT catalysts. The catalysts with higher acidity and larger size of Ru particle (Ru/CNT-C623-H623 with a mean Ru size of 8.7 nm and Ru/CNT-C623-H773 with a mean Ru size of 12 nm) afforded higher sorbitol selectivity. We speculate that the higher acidity which could provide higher rate of 3-β-D-glucopyranosyl-D-glucitol conversions (Table 6) and the lower rate of large Ru particles in sorbitol degradation both contribute to the higher sorbitol selectivity over these catalysts. To further confirm this speculation, we have carried out conversions of sorbitol over different Ru/CNT catalysts.

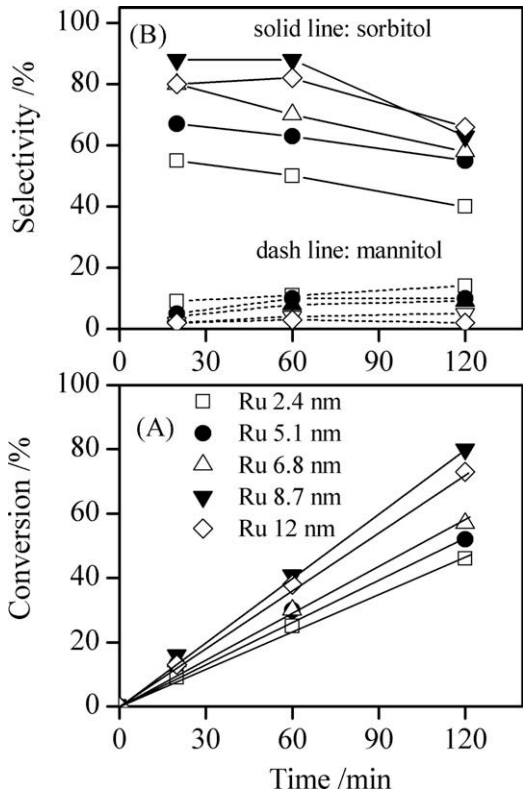

Fig. 13. Catalytic behaviors for the conversion of 3-β-D-glucopyranosyl-D-glucitol over the Ru/CNT catalysts with different mean sizes of Ru particles. (A) Conversion and (B) selectivity. Reaction conditions: 3-β-D-glucopyranosyl-D-glucitol, 0.174 mmol; catalyst, 0.050 g; H_2O, 20 cm^3; H_2, 5 MPa; temperature, 458 K.

Table 6
Rate for 3-β-D-glucopyranosyl-D-glucitol conversions over the Ru/CNT catalysts with different mean sizes of Ru particles.

Catalyst	Mean size of Ru (nm)	3-β-D-Glucopyranosyl-D-glucitol conversion rate[a] (mmol g_{cat}^{-1} h^{-1})
Ru/CNT-H773	2.4	71.3
Ru/CNT-EG483	5.1	90.5
Ru/CNT-EG453	6.8	99.2
Ru/CNT-C623-H623	8.7	139
Ru/CNT-C623-H773	12	127

[a] Calculated using the data in Fig. 13A.

Table 7
Conversion of sorbitol over the Ru/CNT catalysts with different mean sizes of Ru particles.[a]

Catalyst	Mean size of Ru (nm)	Reaction time (h)	Conversion[b] (%)
Ru/CNT-H773	2.4	1	25
Ru/CNT-EG483	5.1	1	12
Ru/CNT-C623-H623	8.7	1	4
Ru/CNT-H773	2.4	3	45
Ru/CNT-EG483	5.1	3	23
Ru/CNT-C623-H623	8.7	3	4

[a] Reaction conditions: sorbitol, 1.0 mmol; catalyst, 0.050 g; H_2, 5 MPa; H_2O, 20 cm^3; temperature, 458 K.
[b] The products include mannitol, degradation compounds, and some unknown products.

The results shown in Table 7 revealed that the conversion of sorbitol proceeded significantly faster over the catalysts with smaller sizes of Ru particles, forming mannitol and other degradation products. In other words, sorbitol was more stable over the catalyst with a larger mean size of Ru particles (e.g., 8.7 nm).

In a previous communication [13], protons generated by the autoprotolysis of water were proposed to participate in the hydrolysis of β-1,4-glycosidic bond in hot water. Thus, we have also investigated the conversions of 3-β-D-glucopyranosyl-D-glucitol without any catalyst in hot water and over the CNTs with different post-treatments. These results are compared with those over the Ru/CNT catalysts under the same reaction conditions in Table 8. Indeed, 3-β-D-glucopyranosyl-D-glucitol could be converted to sorbitol, glucose, and HMF with yields of 22%, 13%, and 1%, respectively, in the blank reaction. The use of CNTs with different post-treatments as catalysts further raised the conversion of 3-β-D-glucopyranosyl-D-glucitol and the yield of sorbitol and glucose, suggesting that the acidic sites over the CNTs played roles in the conversion of 3-β-D-glucopyranosyl-D-glucitol. The conversions of 3-β-D-glucopyranosyl-D-glucitol further increased over the Ru/CNT catalysts. This is in consistent with the experimental result that the Ru/CNT catalysts exhibit higher acidity than CNTs (Table 1). However, no glucose was obtained over the Ru/CNT, further confirming that glucose could be transformed to sorbitol very rapidly over the Ru nanoparticles. Only the catalysts with larger-sized Ru particles (7.8 and 12 nm) could provide higher sorbitol yield (Table 8).

The results described earlier suggest that the catalysts with smaller Ru particles favor the hydrogenolysis of cellobiose to form 3-β-D-glucopyranosyl-D-glucitol (Step I in Fig. 11). Moreover, these catalysts are detrimental to keeping sorbitol from degradation (Steps IV and V in Fig. 11). Therefore, it is understandable that the catalysts with smaller mean sizes of Ru particles (<8.7 nm) can achieve higher yields of 3-β-D-glucopyranosyl-D-glucitol in a short reaction time but are less efficient for sorbitol formation (Fig. 9). On the other hand, over the catalysts with larger Ru particles (8.7 and 12 nm), the higher acidity of these catalysts is beneficial for forming sorbitol through the cleavage of the β-1,4-glycosidic bond of 3-β-D-glucopyranosyl-D-glucitol. The lower degradation rate of sorbitol over the larger Ru particles is also an important factor for obtaining the high yield of sorbitol over these catalysts. In short, our results suggest that, for an efficient conversion of cellobiose to sorbitol, we should consider not only the size of Ru particles, which may play key roles in the hydrogenolysis step and degradation of the target product, but also the acidic properties of the catalysts, which are crucial for the conversion of 3-β-D-glucopyranosyl-D-glucitol. We hope that these insights may be helpful for the design of efficient catalysts for the transformation of cellulose. Detailed mechanistic studies on cellulose conversions are underway.

4. Conclusions

The Ru/CNT can efficiently catalyze the direct conversion of cellobiose into sorbitol in the presence of hydrogen in neutral water medium. A sorbitol yield of 87% has been attained at 458 K. The mean size of Ru nanoparticles and the acidity of the catalysts are key factors dominating the catalytic performances. The CNTs pretreated by concentrated nitric acid possess higher concentrations of acidic functional groups and are better catalyst support of Ru catalyst for sorbitol formation. The catalyst with a larger mean size of Ru nanoparticles ($\geqslant$8.7 nm) and higher acidity exhibits a better sorbitol yield, while that with a smaller mean Ru size and lower acidity can afford a better yield of 3-β-D-glucopyranosyl-D-glucitol (as high as 93% at the initial reaction stage). It is elucidated that the reaction involves two key steps. In the first step, cellobiose is transformed into 3-β-D-glucopyranosyl-D-glucitol via the hydrogenoly-

Table 8
Catalytic performances of the CNTs after different post-pretreatments and the Ru/CNT catalysts with different mean sizes of Ru particles for the conversions of 3-β-D-glucopyranosyl-D-glucitol.[a]

Sample	Mean size of Ru (nm)	Conversion (%)	Yield (%)		
			Sorbitol	Glucose	HMF
Blank	–	48	22	13	1
CNT-H773	–	71	26	16	3
CNT-EG483	–	78	32	20	3.5
CNT-EG453	–	78	38	20	4
CNT-C623-H623	–	84	32	11	3
CNT-C623-H773	–	82	41	17	6
Ru/CNT-H773	2.4	83	13	0	0
Ru/CNT-EG483	5.1	87	34	0	0
Ru/CNT-EG453	6.8	88	36	0	0
Ru/CNT-C623-H623	8.7	98	60	0	0
Ru/CNT-C623-H773	12	90	58	0	0

[a] Reaction conditions: 3-β-D-glucopyranosyl-D-glucitol, 0.174 mmol; catalyst, 0.050 g; H_2O, 20 cm^3; H_2, 5 MPa; temperature, 458 K; time, 3 h.

sis of C—O bond in one glucose ring, and then the hydrolysis of the β-1,4 glycosidic bond in 3-β-D-glucopyranosyl-D-glucitol affords sorbitol in the second step. The catalyst with a smaller mean size of Ru particles favors the hydrogenolysis of cellobiose to 3-β-D-glucopyranosyl-D-glucitol. However, it is less active in the subsequent hydrolysis of 3-β-D-glucopyranosyl-D-glucitol into sorbitol due to the lower acidity and being detrimental to keeping sorbitol from degradation. Both the size of Ru nanoparticles and the acidity of catalyst should be considered for an efficient conversion of cellobiose into sorbitol.

Acknowledgments

This work was supported by the National Natural Science Foundation of China (Nos. 20625310, 20873110 and 20923004), the National Basic Program of China (2010CB732303 and 2005CB221408), and the Key Scientific Project of Fujian Province (2009HZ0002-1). We thank Profs. H.B. Zhang and G.D. Lin for providing CNT.

References

[1] G.W. Huber, S. Iborra, A. Corma, Chem. Rev. 107 (2007) 2411.
[2] J.N. Chheda, G.W. Huber, J.A. Dumesic, Angew. Chem. Int. Ed. 46 (2007) 7164.
[3] C.H. Christensen, J. Rass-Hansem, C.C. Marsden, E. Taarning, K. Egeblad, ChemSusChem 1 (2008) 283.
[4] D.A. Simonetti, J.A. Dumesic, Catal. Rev. Sci. Eng. 51 (2009) 441.
[5] D. Klemm, B. Heublein, H.-P. Fink, A. Bohn, Angew. Chem. Int. Ed. 44 (2005) 3358.
[6] A.J. Ragauskas, C.K. Williams, B.H. Davison, G. Britovsek, J. Cairney, C.A. Eckert, W.J. Frederick Jr., J.P. Hallett, D.J. Leak, C.L. Liotta, J.R. Mielenz, R. Murphy, R. Templer, T. Tschaplinski, Science 311 (2006) 484.
[7] P.L. Dhepe, A. Fukuoka, ChemSusChem 1 (2008) 969.
[8] M. Stöcker, Angew. Chem. Int. Ed. 47 (2008) 9200.
[9] K. Fleming, D.G. Gray, S. Matthews, Chem. Eur. J. 7 (2001) 1831.
[10] Y. Nishiyama, P. Langan, H. Chanzy, J. Am. Chem. Soc. 124 (2002) 9074; Y. Nishiyama, J. Sugiyama, H. Chanzy, P. Langan, J. Am. Chem. Soc. 125 (2003) 14300.
[11] B. Kamm, Angew. Chem. Int. Ed. 46 (2007) 5056.
[12] A. Fukuoka, P.L. Dhepe, Angew. Chem. Int. Ed. 45 (2006) 5161.
[13] C. Luo, S. Wang, H. Liu, Angew. Chem. Int. Ed. 46 (2007) 7636.
[14] N. Ji, T. Zhang, M. Zheng, A. Wang, H. Wang, X. Wang, J.G. Chen, Angew. Chem. Int. Ed. 47 (2008) 8510.
[15] Y. Su, H.M. Brown, X. Huang, A.-D. Zhou, J.E. Amonette, Z.C. Zhang, Appl. Catal. A 361 (2009) 117.
[16] W. Deng, X. Tan, W. Fang, Q. Zhang, Y. Wang, Catal. Lett. 133 (2009) 167.
[17] N. Yan, C. Zhao, C. Luo, P.J. Dyson, H. Liu, Y. Kou, J. Am. Chem. Soc. 128 (2006) 8714.
[18] J.A. Bootsma, B.H. Shanks, Appl. Catal. A 327 (2007) 44.
[19] P. Gallezot, N. Nicolaus, G. Flèche, P. Fuertes, A. Perrard, J. Catal. 180 (1998) 51.
[20] B.W. Hoffer, E. Crezee, P.R.M. Mooijman, A.D. Langeveld, F. Kapteijn, J.A. Moulijn, Catal. Today 79 (2003) 35.
[21] J. Pan, J. Li, C. Wang, Z. Yang, React. Kinet. Catal. Lett. 90 (2007) 233.
[22] P. Chen, H.B. Zhang, G.D. Lin, Q. Hong, K.R. Tsai, Carbon 35 (1997) 1495.
[23] A.J. Plomp, D.S. Su, K.P. de Jong, J.H. Bitter, J. Phys. Chem. C 113 (2009) 9865.
[24] A. Miyazaki, I. Balint, K. Aika, Y. Nakano, J. Catal. 204 (2001) 364.
[25] K.C. Taylor, J. Catal. 38 (1975) 299.
[26] P. Serp, M. Corrias, P. Kalck, Appl. Catal. A 253 (2003) 337.
[27] J.F. Moulder, W.F. Stickle, P.E. Sobol, K.D. Bomben, Handbook of X-ray Photoelectron Spectroscopy, Physical Electronics, Inc., Eden Prairie, 1995.
[28] F. Li, J. Chen, Q. Zhang, Y. Wang, Green Chem. 10 (2008) 553.
[29] J. Kang, S. Zhang, Q. Zhang, Y. Wang, Angew. Chem. Int. Ed. 48 (2009) 2565.
[30] G.A. Somorjai, J.Y. Park, Top. Catal. 49 (2008) 126.
[31] U. Zielke, K.J. Hüttinger, W.P. Hoffman, Carbon 34 (1996) 983.
[32] P.V. Laksgminarayanan, H. Toghiani, C.U. Pittman Jr., Carbon 42 (2004) 2433.
[33] T.I.T. Okpalugo, P. Papakonstantinou, H. Murphy, J. McLaughlin, N.M.D. Brown, Carbon 43 (2005) 153.
[34] J. Álvarez-Rodríguez, A. Guerrero-Ruiz, I. Rodríguez-Ramos, A. Arcoya-Martín, Catal. Today 107 (2005) 302.